

Linear Theory of Thin, Radially-Stratified Disks

Bryan M. Johnson and Charles F. Gammie

Center for Theoretical Astrophysics, University of Illinois at Urbana-Champaign, 1110 West Green St., Urbana, IL 61801

ABSTRACT

We consider the nonaxisymmetric linear theory of radially-stratified disks. We work in a shearing-sheet-like approximation, where the vertical structure of the disk is neglected, and develop equations for the evolution of a plane-wave perturbation comoving with the shear flow (a shearing wave, or “shwave”). We calculate a complete solution set for compressive and incompressive short-wavelength perturbations in both the stratified and unstratified shearing-sheet models. We develop expressions for the late-time asymptotic evolution of an individual shwave as well as for the expectation value of the energy for an ensemble of shwaves that are initially distributed isotropically in k -space. We find that: (i) incompressive, short-wavelength perturbations in the unstratified shearing sheet exhibit transient growth and asymptotic decay, but the energy of an ensemble of such shwaves is constant with time (consistent with Afshordi, Mukhopadhyay, & Narayan 2004); (ii) short-wavelength compressive shwaves grow asymptotically in the unstratified shearing sheet, as does the energy of an ensemble of such shwaves; (iii) incompressive shwaves in the stratified shearing sheet have density and azimuthal velocity perturbations $\delta\Sigma$, $\delta v_y \sim t^{-\text{Ri}}$ (for $|\text{Ri}| \ll 1$), where $\text{Ri} \equiv N_x^2/(\tilde{q}\Omega)^2$ is the Richardson number, N_x^2 is the square of the radial Brunt-Väisälä frequency and $\tilde{q}\Omega$ is the effective shear rate; (iv) the energy of an ensemble of incompressive shwaves in the stratified shearing sheet behaves asymptotically as $\text{Ri} t^{1-4\text{Ri}}$ for $|\text{Ri}| \ll 1$. For Keplerian disks with modest radial gradients, $|\text{Ri}|$ is expected to be $\ll 1$, and there will therefore be weak growth in a single shwave for $\text{Ri} < 0$ and near-linear growth in the energy of an ensemble of shwaves, independent of the sign of Ri .

Subject headings: accretion, accretion disks, solar system: formation, galaxies: nuclei

1. Introduction

Angular momentum transport is central to the evolution of astrophysical disks. In many disks angular momentum is likely redistributed internally by magnetohydrodynamic (MHD) turbulence driven by the magnetorotational instability (MRI; see Balbus & Hawley 1998). But in portions of disks around young, low-mass stars, in cataclysmic-variable disks in quiescence, and in X-ray transients in quiescence (Stone, Gammie, Balbus, & Hawley 2000; Gammie & Menou 1998; Menou

2000), disks may be composed of gas that is so neutral that the MRI fails. It is therefore of interest to understand if there are purely hydrodynamic mechanisms for driving turbulence *and* angular momentum transport in disks.

The case for hydrodynamic angular momentum transport is not promising. Numerical experiments carried out under conditions similar to those under which the MRI produces ample angular momentum fluxes—local shearing-box models—show small or negative angular momentum fluxes when the magnetic field is turned off (Hawley, Gammie, & Balbus 1995; Hawley, Gammie, & Balbus 1996). Unstratified shearing-sheet models show decaying angular momentum flux and kinetic energy when nonlinearly perturbed, yet recover the well known, high Reynolds number nonlinear instability of plane Couette flow when the parameters of the model are set appropriately (Balbus, Hawley, & Stone 1996; see, however, the recent results by Umurhan & Regev 2004). Local models with unstable vertical stratification show overturning and the development of convective turbulence, but the mean angular momentum flux is small and of the wrong sign (Stone & Balbus 1996).

Linear theory of global disk models has long indicated the presence of instabilities associated with reflecting boundaries or features in the flow (see e.g., Papaloizou & Pringle 1984, 1985, 1987; Goldreich, Goodman, & Narayan 1986; Goodman, Narayan, & Goldreich 1987; Narayan, Goldreich, & Goodman 1987; Lovelace, Li, Colgate, & Nelson 1999; Li, Finn, Lovelace, & Colgate 2000). Numerical simulations of the nonlinear outcome of these instabilities suggest that they saturate at low levels and are turned off by modest accretion (Blaes 1987; Hawley 1991). One might guess that in the nonlinear outcome these instabilities will attempt to smooth out the features that give rise to them, much as convection tends to erase its parent entropy gradient. There are some suggestions, however, that such instabilities saturate into long-lived vortices, which may serve as obstructions in the flow that give rise to angular momentum transport (Li, Colgate, Wendroff, & Liska 2001). We will consider this possibility in a later publication.

Linear theory has yet to uncover a *local* instability of hydrodynamic disks that produces astrophysically-relevant angular momentum fluxes. Because of the absence of a complete set of modes in the shearing-sheet model, however, local linear stability is difficult to prove. Local nonlinear stability may be impossible to prove. Comparison with laboratory Couette flow experiments is complicated by several factors, not least of which is the inevitable presence of solid radial boundaries in the laboratory that have no analogue in astrophysical disks.

Recently, however, Klahr & Bodenheimer (2003) (hereafter KB03) have claimed to find a local hydrodynamic instability in global numerical simulations. The instability arises in a model with scale-free initial conditions (an equilibrium entropy profile that varies as a power-law in radius) and thus does not depend on sharp features in the flow. Klahr (2004) has performed a local linear stability analysis of a radially-stratified accretion disk in an effort to explain the numerical results obtained by KB03. The instability mechanism invoked is the phenomenon of transient amplification as a shearing wave goes from leading to trailing. This is the mechanism that operates for nonaxisymmetric shearing waves in a disk that is nearly unstable to the axisymmetric gravitational

instability (Goldreich & Lynden-Bell 1965; Julian & Toomre 1966; Goldreich & Tremaine 1978). It is the purpose of this work to clarify and extend the linear analysis of Klahr (2004). If this instability exists it could be important for the evolution of low-ionization disks.

To isolate the cause for instabilities originally observed in global 3D simulations, KB03 perform both local and global 2D calculations in the (R, ϕ) -plane. The local simulations use a new set of boundary conditions termed the shearing-disk boundary conditions. The model is designed to simulate a local portion of the disk without neglecting global effects such as curvature and horizontal flow gradients. The boundary conditions, which are described in more detail in KB03, require the assumption of a power-law scaling for the mean values of each of the variables, as well as the assumption that the fluctuations in each variable are proportional to their mean values. The radial velocity component in the inner and outer four grid cells is damped by 5% each time step in order to remove artificial radial oscillations produced by the model.¹

The equilibrium profile for KB03’s 2D runs was a constant surface density Σ with either a constant temperature T or a temperature profile $T \propto R^{-1}$. The constant- T runs showed no instability while those with varying T (and thus varying entropy) sustained turbulence and positive Reynolds stresses.² The fiducial local simulations were run at a resolution of 64^2 , with a spatial domain of $R = 4$ to 6 AU and $\Delta\phi = 30^\circ$. The unstable run was repeated at a resolution of 128^2 , along with a run at twice the physical size of the fiducial runs. One global model (with non-reflecting outflow boundary conditions) was run at a resolution of 128^2 with a spatial domain of $R = 1$ to 10 AU and $\Delta\phi = 360^\circ$. All the runs yielded similar results, with the larger simulations producing vortices and power on large scales.

KB03 have chosen the term “baroclinic instability” by way of analogy with the baroclinic instability that gives rise to weather patterns in the atmosphere of the Earth and other planets (see e.g. Pedlosky 1979).³ The analogy is somewhat misleading, however, since the baroclinic instability that arises in planetary contexts is due to a baroclinic equilibrium. In a planetary atmosphere, a baroclinically-unstable situation requires stratification in both the vertical and latitudinal directions.⁴ The stratification in KB03 is only in the radial direction, and as a result the equilibrium is barotropic. It is the perturbations that are baroclinic; i.e., the disk is only baroclinic at linear order in the amplitude of a disturbance.

¹It is not surprising that shearing disk boundary conditions as implemented in KB03 produce features on the radial boundary, because the Coriolis parameter is discontinuous across the radial boundary.

²Notice that with a constant Σ , the constant- T runs have no variation in any of the equilibrium variables, so it is not clear that the effects being observed in the 2D calculations are due to the presence of an entropy gradient rather than due simply to the presence of a pressure gradient.

³A baroclinic flow is one in which surfaces of constant density are inclined with respect to surfaces of constant pressure. If these surfaces coincide, the flow is termed barotropic.

⁴Contrary to the claim in Klahr (2004), the two-layer model (Pedlosky 1979) does not ignore the vertical structure; it simply considers the lowest-order vertical mode.

Cabot (1984) and Knobloch & Spruit (1986) have analyzed a thin disk with a baroclinic equilibrium state (with both vertical and radial gradients). The latter find that due to the dominant effect of the Keplerian shear, the instability only occurs if the radial scale height is comparable to the vertical scale height, a condition which is unlikely to be astrophysically relevant. As pointed out in KB03, the salient feature that is common to their analysis and the classical baroclinic instability is an equilibrium entropy gradient in the horizontal direction. As we show in §2, however, an entropy gradient is not required in order for two-dimensional perturbations to be baroclinic; any horizontal stratification will do.

The “global baroclinic instability” claimed by KB03 is thus analogous to the classical baroclinic instability in the sense that both have the potential to give rise to convection.⁵ When neglecting vertical structure, however, the situation in an accretion disk is more closely analogous to a shearing, stratified atmosphere, the stability of which is governed by the classical Richardson criterion (Miles 1961; Chimonas 1970). The only additional physics in a disk is the presence of the Coriolis force. Most analyses of a shearing, stratified atmosphere, however, only consider stratification profiles that are stable to convection. The primary question that Klahr (2004) and this work are addressing, then, is whether or not the presence of shear stabilizes a stratified equilibrium that would be unstable in its absence.

We begin in §2 by outlining the basic equations for a local model of a thin disk. §§3 and 4 describe the local linear theory for nonaxisymmetric sinusoidal perturbations in unstratified and radially-stratified disks, respectively. We summarize and discuss the implications of our findings in §5.

2. Basic Equations

The effect of radial gradients on the local stability of a thin disk can be analyzed most simply in the two-dimensional shearing-sheet approximation. This is obtained by a rigorous expansion of the equations of motion in the ratio of the vertical scale height H to the local radius R , followed by a vertical integration of the fluid equations. The basic equations that one obtains (e.g., Goldreich & Tremaine 1978) are

$$\frac{d\Sigma}{dt} + \Sigma \nabla \cdot \mathbf{v} = 0, \quad (1)$$

$$\frac{d\mathbf{v}}{dt} + \frac{\nabla P}{\Sigma} + 2\Omega \times \mathbf{v} - 2q\Omega^2 x \hat{\mathbf{x}} = 0, \quad (2)$$

$$\frac{d \ln S}{dt} = 0, \quad (3)$$

⁵The classical baroclinic instability gives rise to a form of “sloping convection” (Houghton 2002) since the latitudinal entropy gradient is inclined with respect to the vertical buoyancy force.

where Σ and P are the two-dimensional density and pressure, $S \equiv P\Sigma^{-\gamma}$ is monotonically related to the fluid entropy,⁶ \mathbf{v} is the fluid velocity and d/dt is the Lagrangian derivative. The third and fourth terms in equation (2) represent the Coriolis and centrifugal forces in the local model expansion, where Ω is the local rotation frequency, x is the radial Cartesian coordinate and q is the shear parameter (equal to 1.5 for a disk with a Keplerian rotation profile). The gravitational potential of the central object is included as part of the centrifugal force term in the local-model expansion, and we ignore the self-gravity of the disk.

It is worth emphasizing at this point that we have integrated out the vertical degrees of freedom in the model. We will later focus on perturbations with planar wavelengths that are small compared to a scale height, and these perturbations will be strongly influenced by the vertical structure of the disk.

Equations (1) through (3) can be combined into a single equation governing the evolution of the potential vorticity:

$$\frac{d}{dt} \left(\frac{\nabla \times \mathbf{v} + 2\Omega}{\Sigma} \right) \equiv \frac{d\xi}{dt} = \frac{\nabla \Sigma \times \nabla P}{\Sigma^3}. \quad (4)$$

In two dimensions, ξ has only one nonzero component and can therefore be regarded as a scalar. Equation (4) demonstrates that for $P \equiv P(\Sigma)$ (as in the case of a strictly adiabatic evolution with isentropic initial conditions), the potential vorticity of fluid elements is conserved. For $P \neq P(\Sigma)$, however, the potential vorticity evolves with time. A barotropic equilibrium stratification can result in baroclinic perturbations that cause the potential vorticity to evolve at linear order. This can be seen by linearizing the scalar version of equation (4):

$$\frac{\partial \delta\xi}{\partial t} + \mathbf{v}_0 \cdot \nabla \delta\xi + \delta\mathbf{v} \cdot \nabla \xi_0 = \frac{\hat{\mathbf{z}} \cdot (\nabla \Sigma_0 \times \nabla \delta P - \nabla P_0 \times \nabla \delta \Sigma)}{\Sigma_0^3}, \quad (5)$$

where we have dropped the term $\propto \nabla \Sigma_0 \times \nabla P_0$. Notice that an entropy gradient is not required for the evolution of the perturbed potential vorticity. For $S_0 = P_0 \Sigma_0^\gamma = \text{constant}$, equation (5) reduces to

$$\frac{\partial \delta\xi}{\partial t} + \mathbf{v}_0 \cdot \nabla \delta\xi + \delta\mathbf{v} \cdot \nabla \xi_0 = \frac{\hat{\mathbf{z}} \cdot (\nabla P_0 \times \nabla \delta S)}{\gamma \Sigma_0^2 S_0}. \quad (6)$$

Potential vorticity is conserved only in the limit of zero stratification ($P_0 = \text{constant}$) or adiabatic perturbations ($\delta S = 0$).

3. Unstratified Shearing Sheet

Our goal is to understand the effects of radial stratification, but we begin by developing the linear theory of the standard (unstratified) shearing sheet, in which the equilibrium density and

⁶With the assumptions of vertical hydrostatic equilibrium and negligible self-gravity, the effective two-dimensional adiabatic index can be shown to be $\gamma = (3\gamma_{3D} - 1)/(\gamma_{3D} + 1)$ (e.g. Goldreich, Goodman, & Narayan 1986).

pressure are assumed to be spatially constant. This will serve to establish notation and method of analysis and to highlight the changes introduced by radial stratification in the next section.

Our analysis follows that of Goldreich & Tremaine (1978) except for our neglect of self-gravity. The equilibrium consists of a uniform sheet with $\Sigma = \Sigma_0 = \text{constant}$, $P = P_0 = \text{constant}$, and $\mathbf{v}_0 = -q\Omega x\hat{\mathbf{y}}$. We consider nonaxisymmetric Eulerian perturbations about this equilibrium with space-time dependence $\delta(t)\exp(ik_x(t)x + ik_y y)$, where

$$k_x(t) \equiv k_{x0} + q\Omega k_y t \quad (7)$$

(with k_{x0} and $k_y > 0$ constant) is required to allow for a spatial Fourier decomposition of the perturbation. We will refer to these perturbations as shearing waves, or with some trepidation, but more compactly, as *shwaves*.

3.1. Linearized Equations

To linear order in the perturbation amplitudes, the dynamical equations reduce to

$$\frac{\dot{\delta\Sigma}}{\Sigma_0} + ik_x\delta v_x + ik_y\delta v_y = 0, \quad (8)$$

$$\dot{\delta v_x} - 2\Omega\delta v_y + ik_x\frac{\delta P}{\Sigma_0} = 0, \quad (9)$$

$$\dot{\delta v_y} + (2 - q)\Omega\delta v_x + ik_y\frac{\delta P}{\Sigma_0} = 0, \quad (10)$$

$$\frac{\dot{\delta P}}{\Sigma_0} + c_s^2(ik_x\delta v_x + ik_y\delta v_y) = 0, \quad (11)$$

where $c_s^2 = \gamma P_0/\Sigma_0$ is the square of the equilibrium sound speed and an over-dot denotes a time derivative.

The above system of equations admits four linearly-independent solutions. Two of these are the non-vortical shwaves (solutions for which the perturbed potential vorticity is zero), which in the absence of self-gravity can be solved for exactly. The remaining two solutions are the vortical shwaves. When $k_y \rightarrow 0$ the latter reduce to the zero-frequency modes of the axisymmetric version of equations (8) through (11). One of these (the entropy mode) remains unchanged in nonaxisymmetry (in a frame comoving with the shear). There is thus only one nontrivial vortical shwave in the unstratified shearing sheet.

In the limit of tightly-wound shwaves ($|k_x| \gg k_y$), the nonvortical and vortical shwaves are compressive and incompressive, respectively. In the short-wavelength limit ($Hk_y \gg 1$, where $H \equiv c_s/\Omega$ is the vertical scale height), the compressive and incompressive solutions remain well separated at all times, but for $Hk_y \lesssim O(1)$ there is mixing between them near $k_x = 0$ as an

incompressive shwave shears from leading to trailing.⁷ With the understanding that the distinction between compressive shwaves and incompressive shwaves as separate solutions is not valid for all time when $Hk_y \lesssim O(1)$, we generally choose to employ these terms over the more general but less intuitive terms “non-vortical” and “vortical.”

Based upon the above considerations, it is convenient to study the vortical shwave in the short-wavelength, low-frequency ($\partial_t \ll c_s k_y$) limit. This is equivalent to working in the Boussinesq approximation,⁸ which in the unstratified shearing sheet amounts to assuming incompressible flow. In this limit, equation (8) is replaced with

$$k_x \delta v_x + k_y \delta v_y = 0. \quad (12)$$

This demonstrates the incompressive nature of the vortical shwave in the short-wavelength limit.

3.2. Solutions

In the unstratified shearing sheet, equation (5) for the perturbed potential vorticity can be integrated to give:

$$\delta \xi_u = \frac{ik_x \delta v_y - ik_y \delta v_x}{\Sigma_0} - \xi_0 \frac{\delta \Sigma}{\Sigma_0} = \text{constant}, \quad (13)$$

where $\xi_0 = (2 - q)\Omega/\Sigma_0$ is the equilibrium potential vorticity and we have employed the subscript u to highlight the fact that the perturbed potential vorticity is only constant in the unstratified shearing sheet. To obtain the compressive-shwave solutions, we set the constant $\delta \xi_u$ to zero. Combining equations (10) and (13) with $\delta \xi_u = 0$, one obtains an expression for δv_{xc} in terms of δv_{yc} and its derivative:

$$\delta v_{xc} = \frac{c_s^2 k_x k_y \delta v_{yc} - \xi_0 \Sigma_0 \delta \dot{v}_{yc}}{\xi_0^2 \Sigma_0^2 + c_s^2 k_y^2}, \quad (14)$$

where the subscript c indicates a compressive shwave. The associated density and pressure perturbations are

$$\delta \Sigma_c = \frac{\delta P_c}{c_s^2} = i \frac{\xi_0 \Sigma_0 k_x \delta v_{yc} + k_y \delta \dot{v}_{yc}}{\xi_0^2 \Sigma_0^2 + c_s^2 k_y^2} \quad (15)$$

via equation (13). Reinserting equation (14) into equation (10), taking one time derivative and replacing $\delta \dot{P}$ via equation (11), we obtain the following remarkably simple equation:

$$\ddot{\delta v}_{yc} + (c_s^2 k^2 + \kappa^2) \delta v_{yc} = 0, \quad (16)$$

where $k^2 = k_x^2 + k_y^2$ and $\kappa^2 = (2 - q)\Omega^2$ is the epicyclic frequency. Changing to the dimensionless dependent variable

$$T \equiv i \sqrt{\frac{2c_s k_y}{q\Omega}} \left(q\Omega t + \frac{k_{x0}}{k_y} \right) \equiv i \sqrt{\frac{2c_s k_y}{q\Omega}} \tau \quad (17)$$

⁷This was pointed out to us by J. Goodman.

⁸We demonstrate this equivalence in the Appendix.

and defining

$$C \equiv \frac{c_s^2 k_y^2 + \kappa^2}{2q\Omega c_s k_y}, \quad (18)$$

the equation governing δv_{yc} becomes

$$\frac{d^2 \delta v_{yc}}{dT^2} + \left(\frac{1}{4} T^2 - C \right) \delta v_{yc} = 0. \quad (19)$$

This is the parabolic cylinder equation (e.g. Abramowitz & Stegun 1972), the solutions of which are parabolic cylinder functions. One representation of the general solution is

$$\delta v_{yc} = e^{-\frac{i}{2}T^2} \left[c_1 M \left(\frac{1}{4} - \frac{i}{2}C, \frac{1}{2}, \frac{i}{2}T^2 \right) + c_2 T M \left(\frac{3}{4} - \frac{i}{2}C, \frac{3}{2}, \frac{i}{2}T^2 \right) \right], \quad (20)$$

where c_1 and c_2 are constants of integration and M is a confluent hypergeometric function. This completely specifies the compressive solutions for the unstratified shearing sheet, for any value of k_y .

Equation (19) has been analyzed in detail by Narayan, Goldreich, & Goodman (1987); their modal analysis yields the analogue of equation (19) in radial-position space rather than in the radial-wavenumber ($k_x = k_y \tau$) space that forms the natural basis for our shwave analysis. One way of seeing the correspondence between the modes and shwaves is to take the Fourier transform of the asymptotic form of the solution. Appropriate linear combinations of the solutions given in equation (20) have the following asymptotic time dependence for $\tau \gg 1$:

$$\delta v_{yc} \propto \sqrt{\frac{2}{T}} \exp \left(\pm \frac{i}{4} T^2 \right) \propto \frac{1}{\sqrt{k_x}} \exp \left(\pm i \int c_s k_x dt \right). \quad (21)$$

The Fourier transform of the above expression, evaluated by the method of stationary phase for $Hk_y \gg 1$, yields

$$\delta v_{yc}(X) \propto \sqrt{\frac{2}{X}} \exp \left(\pm \frac{i}{4} X^2 \right), \quad (22)$$

which is equivalent to the expressions given for the modes analyzed by Narayan, Goldreich, & Goodman (1987), in which the dimensionless spatial variable (with zero frequency, so that corotation is at $x = 0$) is defined as

$$X \equiv \sqrt{\frac{2q\Omega k_y}{c_s}} x. \quad (23)$$

To obtain the incompressive shwave, we use the condition of incompressibility (equation (12)) to write δv_y in terms of δv_x , and then combine the dynamical equations (9) and (10) to eliminate δP . The incompressive shwave is given by:

$$\delta v_{xi} = \delta v_{xi0} \frac{k_0^2}{k^2}, \quad (24)$$

$$\delta v_{yi} = -\frac{k_x}{k_y} \delta v_{xi}, \quad (25)$$

$$\frac{\delta \Sigma_i}{\Sigma_0} = \frac{\delta P_i}{\gamma P_0} = \frac{1}{ic_s k_y} \left(\frac{k_x}{k_y} \frac{\dot{\delta} v_{xi}}{c_s} + 2(q-1)\Omega \frac{\delta v_{xi}}{c_s} \right), \quad (26)$$

where the subscript i indicates an incompressive shwave, $k_0^2 = k_{x0}^2 + k_y^2$ and δv_{xi0} is the value of δv_{xi} at $t = 0$.⁹ This solution is uniformly valid for all time to leading order in $(Hk_y)^{-1} \ll 1$.

3.3. Energetics of the Incompressive Shwaves

We define the kinetic energy in a single incompressive shwave as

$$E_{ki} \equiv \frac{1}{2} \Sigma_0 (\delta v_{xi}^2 + \delta v_{yi}^2) = \frac{1}{2} \Sigma_0 \delta v_{xi}^2 \frac{k^2}{k_y^2} = \frac{1}{2} \Sigma_0 \delta v_{xi0}^2 \frac{k_0^4}{k_y^2 k^2}, \quad (27)$$

which peaks at $k_x = 0$. This is not the only possible definition for the energy associated with a shear-flow disturbance; see the discussion in Appendix A of Narayan, Goldreich, & Goodman (1987).

One can also define an amplification factor for an individual shwave,

$$\mathcal{A} \equiv \frac{E_{ki}(k_x = 0)}{E_{ki}(t = 0)} = 1 + \frac{k_{x0}^2}{k_y^2}, \quad (28)$$

which indicates that an arbitrary amount of transient amplification in kinetic energy can be obtained as one increases the amount of swing for a leading shwave ($k_{x0} \ll -k_y$). This is essentially the mechanism invoked by Chagelishvili, Zahn, Tevzadze, & Lominadze (2003), Umurhan & Regev (2004) and Afshordi, Mukhopadhyay, & Narayan (2004) to argue for the onset of turbulence in unmagnetized Keplerian disks.

Because only a small subset of all Fourier components achieve large amplification (those with initial wavevector very nearly aligned with the radius vector), one must ask what amplification is achieved for an astrophysically relevant set of initial conditions containing a superposition of Fourier components. It is natural to draw such a set of Fourier components from a distribution that is isotropic, or nearly so, when k_0 is large.

Consider, then, perturbing a disk with a random set of incompressive perturbations (initial velocities perpendicular to \mathbf{k}_0) drawn from an isotropic, Gaussian random field and asking how the expectation value for the kinetic energy associated with the perturbations evolves with time. The evolution of the expected energy density is given by the following integral:

$$\langle E_i \rangle = L^2 \int d^2 k_0 \langle E_{ki} \rangle = L^2 \int d^2 k_0 \frac{1}{2} \Sigma_0 \langle \delta v_{xi0}^2 \rangle \frac{k_0^4}{k_y^2 k^2}. \quad (29)$$

⁹Chagelishvili, Zahn, Tevzadze, & Lominadze (2003) obtained this solution by starting with the assumption of incompressibility.

where $\langle \rangle$ indicates an average over an ensemble of initial conditions, the first equality follows from Parseval’s theorem, the second equality follows from the incompressive shwave solution (24)-(26) and therefore applies only for $k_0 H \gg 1$, and L^2 is a normalizing factor with units of length squared.

For initial conditions that are isotropic in \mathbf{k}_0 ($\delta v_{xio} = \delta v_{\perp}(k_0, \theta) \sin \theta$, where $\langle \delta v_{\perp}^2(k_0) \rangle$ is the expectation value for the initial incompressive perturbation as a function of k_0 and $\tan \theta = k_y/k_{x0}$), the integral becomes

$$\langle E_i \rangle = \frac{1}{2} \Sigma_0 L^2 \int k_0 dk_0 \langle \delta v_{\perp}^2(k_0) \rangle \int_0^{2\pi} d\theta \frac{1}{\sin^2 \theta + (q\Omega t \sin \theta + \cos \theta)^2}. \quad (30)$$

Changing integration variables to $\tau = q\Omega t + \cot \theta$, the angular integral becomes

$$\int_{-\infty}^{\infty} d\tau \frac{2}{1 + \tau^2} = 2\pi, \quad (31)$$

which is independent of time; hence

$$\langle E_i \rangle = \langle E_i(t=0) \rangle \quad (32)$$

and we do not expect the total energy in incompressive shwaves to evolve.

Although this result may appear to depend in detail on the assumption of isotropy, one can show that it really only depends on $\langle E_{ki}(t=0) \rangle$ being smooth near $\sin \theta = 0$, i.e. that there should not be a concentration of power in nearly radial wavevectors. This can be seen from the following argument. If we relax the assumption of isotropy, the angular integral becomes

$$\int_0^{2\pi} d\theta \frac{\langle \delta v_{\perp}^2(k_0, \theta) \rangle}{\sin^2 \theta + (q\Omega t \sin \theta + \cos \theta)^2}. \quad (33)$$

For $q\Omega t \gg 1$ the above integrand is sharply peaked in the narrow regions around $\tan \theta = -1/(q\Omega t) \ll 1$ (i.e., $\sin \theta \simeq 0$). One can perform a Taylor-series expansion of $\langle \delta v_{\perp}^2(k_0, \theta) \rangle$ in these regions, and as long as $\langle \delta v_{\perp}^2(k_0, \theta) \rangle$ itself is not sharply peaked it is well approximated as a constant. A modest relaxation of the assumption of isotropy, then, will result in an asymptotically constant value for the energy integral.

Based upon this analysis, large amplification in an individual shwave does not in itself argue for a transition to turbulence due to transient growth. One must also demonstrate that a “natural” set of perturbations can extract energy from the background shear flow. In the case of the unstratified shearing sheet, the energy of a random set of incompressive perturbations remains constant with time. This is consistent with the results of Umurhan & Regev (2004), who see asymptotic decay in linear theory, because they work with a finite set of wavevectors, each of which must decay asymptotically.

3.4. Energetics of the Compressive Shwaves

Here we calculate the energy evolution of the compressive shwaves for comparison purposes. We will consider the evolution of short-wavelength compressive shwaves in which only the initial

velocity is perturbed, both for simplicity and for consistency with our calculation of the short-wavelength incompressive shwaves. As before, we will assume that the initial kinetic energy is distributed isotropically.

We use the WKB solutions to equation (16) with $Hk_y \gg 1$.¹⁰ With the initial density perturbation set to zero (consistent with our assumption of only initial velocity perturbations), the uniformly-valid asymptotic solution to leading order in $(Hk_y)^{-1}$ is given by

$$\delta v_{yc} = \delta v_{yc0} \sqrt{\frac{k_0}{k}} \cos(W - W_0), \quad (34)$$

$$\delta v_{xc} = \frac{k_x}{k_y} \delta v_{yc}, \quad (35)$$

$$\delta \Sigma_c = \frac{i}{c_s^2 k_y} \delta v_{yc}, \quad (36)$$

where the WKB eikonal is given by

$$W \equiv \int c_s k dt = \frac{Hk_y}{q} \int \sqrt{1 + \tau^2} d\tau = \frac{Hk_y}{2q} \left(\tau \sqrt{1 + \tau^2} + \ln \left(\tau + \sqrt{1 + \tau^2} \right) \right), \quad (37)$$

with W_0 being the value of W at $t = 0$.¹¹

Using equation (35), the energy integral for the compressive shwaves in the short-wavelength limit is

$$\langle E_c \rangle = L^2 \int d^2 k_0 \langle E_{kc} \rangle = L^2 \int d^2 k_0 \frac{1}{2} \Sigma_0 \langle \delta v_{yc}^2 \rangle \frac{k^2}{k_y^2}. \quad (38)$$

With initial velocities now parallel to \mathbf{k}_0 (and again isotropic), this becomes

$$\langle E_c \rangle = \frac{1}{2} \Sigma_0 L^2 \int k_0 dk_0 \langle \delta v_{\parallel}^2(k_0) \rangle \int_0^{2\pi} d\theta \sqrt{\sin^2 \theta + (q\Omega t \sin \theta + \cos \theta)^2} \cos^2(W - W_0). \quad (39)$$

For $q\Omega t \gg 1$, the angular integral is approximated by

$$\int_0^{2\pi} d\theta |\sin \theta| (1 + \cos(2W - 2W_0)) \simeq 2q\Omega t + \sqrt{\frac{2\pi q\Omega}{c_s k_0}} \cos(c_s k_0 q\Omega t^2 - \pi/4), \quad (40)$$

where the second approximation comes from employing the method of stationary phase.¹² In the short-wavelength limit, then,

$$\langle E_c(q\Omega t \gg 1) \rangle = 2q\Omega t \langle E_c(t = 0) \rangle. \quad (41)$$

¹⁰These solutions are the short-wavelength, *high*-frequency ($\partial_t \sim O(c_s k_y)$) limit of the full set of linear equations in the shearing sheet; see the Appendix.

¹¹This is not the same WKB solution that is calculated in the tight-winding approximation by Goldreich & Tremaine (1978); in that case $c_s k_y / \kappa \ll 1$, the opposite limit to that which we are considering here. The two WKB solutions match for $\tau \gg 1$ in the absence of self-gravity. We have verified the accuracy of this solution by comparing it to the exact solution with acceptable results, and it is valid to leading order for all time.

¹²The first approximation breaks down near $\sin \theta = 0$, but the contribution of these regions to the integral is negligible for $q\Omega t \gg 1$, in contrast to the situation for incompressive shwaves.

Thus the kinetic energy of an initially isotropic distribution of compressive shwaves grows, presumably at the expense of the background shear flow.

The fate of a single compressive shwave is to steepen into a weak shock train and then decay. The fate of the field of weak shocks generated by an ensemble of compressive shwaves is less clear, but the mere presence of weak shocks does not indicate a transition to turbulence.

4. Radially-Stratified Shearing Sheet

We now generalize our analysis to include the possibility that the background density and pressure varies with x ; this stratification is required for the manifestation of a convective instability. In order to use the shwave formalism we must assume that the background varies on a scale $L \sim H \ll R$ so that the local model expansion (e.g., the neglect of curvature terms in the equations of motion) is still valid.

With this assumption the equilibrium condition becomes

$$\mathbf{v}_0 = \left(-q\Omega x + \frac{P'_0(x)}{2\Omega\Sigma_0(x)} \right) \hat{\mathbf{y}}, \quad (42)$$

where a prime denotes an x -derivative. One can regard the background flow as providing an effective shear rate

$$\tilde{q}\Omega \equiv -v'_0 \quad (43)$$

that varies with x , in which case $\mathbf{v}_0 = -\int^x \tilde{q}(s)ds \Omega \hat{\mathbf{y}}$.

Localized on this background flow we will consider a shearing wave with $k_y L \gg 1$. That is, we will consider nonaxisymmetric short-wavelength Eulerian perturbations with spacetime dependence $\delta(t) \exp(i \int^x \tilde{k}_x(t, s)ds + ik_y y + ik_z z)$, where k_y and k_z are constants and

$$\tilde{k}_x(t, x) \equiv k_{x0} + \tilde{q}(x)\Omega k_y t. \quad (44)$$

It may not be immediately obvious that this is a valid expansion since the shwaves sit on top of a radially-varying background (see Toomre 1969 for a discussion of waves in a slowly-varying background). But this is an ordinary WKB expansion in disguise. To see this, one need only transform to “comoving” coordinates $x' = x$, $y' = y + \int^x \tilde{q}(s)ds \Omega t$, $t' = t$ (this procedure may be more familiar in a cosmological context; as Balbus (1988) has pointed out, this is possible for any flow in which the velocities depend linearly on the spatial coordinates). In this frame the time-dependent wavevector given above is transformed to a time-independent wavevector. The price paid for this is that $\partial_x \rightarrow \partial_{x'} + \tilde{q}\Omega t \partial_{y'}$, so new explicit time dependences appear on the right hand side of the perturbed equations of motion, and the perturbed variables no longer have time dependence $\exp(i\omega t')$. Instead, we must solve an ODE for $\delta(t')$. The y' dependence can be decomposed as $\exp(ik_y y')$. The x' dependence can be treated via WKB, since the perturbation may be assumed

to have the form $W(\epsilon x', \epsilon t') \exp(i\mathbf{k}' \cdot \mathbf{x}')$. This “nearly diagonalizes” the operator $\partial_{x'}$. Thus we are considering the evolution of a wavepacket in comoving coordinates—a “shwavepacket”.

For this procedure to be valid two conditions must be met. First the usual WKB condition must apply, $k_y L \gg 1$. Second, the parameters of the flow that are “seen” by the shwavepacket must change little on the characteristic timescale for variation of $\delta(t)$, which is Ω^{-1} for the incompressive shwaves. For solid body rotation ($\tilde{q} = 0$) the group velocity (derivable from equation (59), below) is $|v_g| < N_x/k$ (for positive squared Brunt-Väisälä frequency N_x^2 , defined below; for $N_x^2 < 0$ the waves grow in place), so the timescale for change of wave packet parameters in this case is $L/|v_g| > kL/N_x \gg \Omega^{-1}$. It seems reasonable to anticipate similarly long timescales when shear is present. As a final check, we have verified directly, using a code based on the ZEUS code of Stone & Norman (1992), that a vortical shwavepacket in the stratified shearing sheet remains localized as it swings from leading to trailing.

4.1. Linearized Equations

To linear order in the perturbation amplitudes, the dynamical equations reduce to

$$\frac{\delta \dot{\Sigma}}{\Sigma_0} + \frac{\delta v_x}{L_\Sigma} + i\tilde{k}_x \delta v_x + ik_y \delta v_y + ik_z \delta v_z = 0, \quad (45)$$

$$\dot{\delta v}_x - 2\Omega \delta v_y + i\tilde{k}_x \frac{\delta P}{\Sigma_0} - \frac{c_s^2}{L_P} \frac{\delta \Sigma}{\Sigma_0} = 0, \quad (46)$$

$$\dot{\delta v}_y + (2 - \tilde{q})\Omega \delta v_x + ik_y \frac{\delta P}{\Sigma_0} = 0, \quad (47)$$

$$\dot{\delta v}_z + ik_z \frac{\delta P}{\Sigma_0} = 0, \quad (48)$$

$$\frac{\delta \dot{P}}{\Sigma_0} - c_s^2 \frac{\delta \dot{\Sigma}}{\Sigma_0} + c_s^2 \frac{\delta v_x}{L_S} = 0, \quad (49)$$

where

$$\frac{1}{L_P} \equiv \frac{P'_0}{\gamma P_0} = \frac{1}{L_\Sigma} + \frac{1}{L_S} \equiv \frac{\Sigma'_0}{\Sigma_0} + \frac{S'_0}{\gamma S_0} \quad (50)$$

define the equilibrium pressure, density and entropy scale heights. We have included the vertical component of the velocity in order to make contact with an axisymmetric convective instability that is present in two dimensions, after which we will set k_z to zero.

We will be mainly interested in the incompressive shwaves because the short-wavelength compressive shwaves are unchanged at leading order by stratification. We will therefore work solely in the Boussinesq approximation.¹³ In addition to the assumption of incompressibility, this approximation considers δP to be negligible in the entropy equation; pressure changes are determined by

¹³We also drop the subscripts distinguishing between the compressive and incompressive shwaves.

whatever is required to maintain nearly incompressible flow. The original Boussinesq approximation applies only to incompressible fluids. It was extended to compressible fluids by Jeffreys (1930) and Spiegel & Veronis (1960). We show in the Appendix that it is formally equivalent to taking the short-wavelength, low-frequency limit of the full set of linear equations. From this viewpoint, assuming that $Hk_y\delta P/P_0$ is of the same order as the other terms in the dynamical equations implies that $\delta P/P_0 \sim (Hk_y)^{-1}\delta\Sigma/\Sigma_0$, thus justifying its neglect in the entropy equation. We therefore replace equations (45) and (49) with

$$\tilde{k}_x\delta v_x + k_y\delta v_y + k_z\delta v_z = 0 \quad (51)$$

and

$$\frac{\dot{\delta\Sigma}}{\Sigma_0} - \frac{\delta v_x}{L_S} = 0. \quad (52)$$

Using equations (47) and (52) and the time derivative of equation (51), one can express $\dot{\delta v}_y$ and δP in terms of δv_x and $\dot{\delta v}_x$:

$$\frac{\delta P}{\Sigma_0} = -i\frac{\tilde{k}_x\dot{\delta v}_x + 2(\tilde{q}-1)\Omega k_y\delta v_x}{k_y^2 + k_z^2}, \quad (53)$$

$$\dot{\delta v}_y = \frac{(-\tilde{q}k_y^2 + (\tilde{q}-2)k_z^2)\Omega\delta v_x - \tilde{k}_xk_y\dot{\delta v}_x}{k_y^2 + k_z^2}. \quad (54)$$

Eliminating δP in equation (46) via equation (53) gives

$$\tilde{k}^2\dot{\delta v}_x + 2(\tilde{q}-1)\Omega\tilde{k}_xk_y\delta v_x = (k_y^2 + k_z^2)(2\Omega\delta v_y + (c_s^2/L_P)\delta\Sigma/\Sigma_0), \quad (55)$$

where $\tilde{k}^2 = \tilde{k}_x^2 + k_y^2 + k_z^2$. Taking the time derivative of this equation and eliminating $\dot{\delta\Sigma}$ and $\dot{\delta v}_y$ via equations (52) and (54), we obtain the following differential equation for δv_x :

$$\tilde{k}^2\ddot{\delta v}_x + 4\tilde{q}\Omega\tilde{k}_xk_y\dot{\delta v}_x + [k_y^2(N_x^2 + 2\tilde{q}^2\Omega^2) + k_z^2(N_x^2 + \tilde{\kappa}^2)]\delta v_x = 0, \quad (56)$$

where $\tilde{\kappa}^2 = 2(2-\tilde{q})\Omega^2$ is the square of the effective epicyclic frequency and

$$N_x^2 \equiv -\frac{c_s^2}{L_S L_P} \quad (57)$$

is the square of the Brunt-Väisälä frequency in the radial direction.¹⁴

¹⁴Notice that N_x^2 , \tilde{q} and $\tilde{\kappa}^2$ are all functions of x and vary on a scale $L \sim H$.

4.2. Comparison with Known Results

Setting $k_y = 0$ in equation (56) yields the axisymmetric modes with the following dispersion relation (for $\delta(t) \propto e^{-i\omega t}$):

$$\omega^2 = \frac{k_z^2}{k_{x0}^2 + k_z^2} (N_x^2 + \tilde{\kappa}^2). \quad (58)$$

This is the origin of the Høiland stability criterion: the axisymmetric modes are stable for $N_x^2 + \tilde{\kappa}^2 > 0$. In the absence of rotation this reduces to the Schwarzschild stability criterion: $N_x^2 > 0$ is the necessary condition for stability. The effect of rotation is strongly stabilizing: if $N_x^2 < -\tilde{\kappa}^2$, as required for instability, then $L_S L_P \sim H^2$; pressure and entropy must vary on radial scales of order the scale height for the disk to be Høiland unstable.

Notice that effective epicyclic frequency $\tilde{\kappa}^2$ only stabilizes modes with nonzero k_z . The stability of nonaxisymmetric shwaves with $k_z = 0$ (as in the mid-plane of a thin disk) is the open question that this work is addressing. In this limit and in the absence of shear the Schwarzschild stability criterion is again recovered: with $k_z = 0$ and $\tilde{q} = 0$ in equation (56) the dispersion relation becomes

$$\omega^2 = \frac{k_y^2}{k_{x0}^2 + k_y^2} N_x^2, \quad (59)$$

If there is a region of the disk where the effective shear is zero, a WKB normal-mode analysis will yield the above dispersion relation and there will be convective instability for $N_x^2 < 0$. It appears from equation (56) that differential rotation provides a stabilizing influence for nonaxisymmetric shwaves just as rotation does for the axisymmetric modes. Things are not as simple in nonaxisymmetry, however. The time dependence is no longer exponential, nor is it the same for all the perturbation variables. There is no clear cutoff between exponential and oscillatory behavior, so the question of flow stability becomes more subtle.

As discussed in the introduction, the Boussinesq system of equations in the shearing-sheet model of a radially-stratified disk bear a close resemblance to the system of equations employed in analyses of a shearing, stratified atmosphere. A sufficient condition for stability in the latter case is that

$$Ri \equiv \frac{N_x^2}{(v'_0)^2} \geq \frac{1}{4} \quad (60)$$

everywhere in the flow, where Ri is the Richardson number, a measure of the relative importance of buoyancy and shear. This stability criterion was originally proved by Miles (1961) and Howard (1961) for incompressible fluids, and its extension to compressible fluids was demonstrated by Chimonas (1970). The stability criterion is based on a normal-mode analysis with rigid boundary conditions. Other than differences in notation (e.g., our radial coordinate corresponds to the vertical coordinate in a stratified atmosphere), the key differences in our system are: (i) the equilibrium pressure gradient in a disk is balanced by centrifugal forces rather than by gravity; (ii) the disk equations contain Coriolis force terms; (iii) most atmospheric analyses only consider an equilibrium that is convectively stable, whereas we are interested in an unstable stratification; (iv) we do not

employ boundary conditions in our analytic model since we are only interested in the possibility of a local instability.

The lack of boundary conditions in our model makes the applicability of the standard Richardson stability criterion in determining local stability somewhat dubious, since the lack of boundary conditions precludes the decomposition of linear disturbances into normal modes. The natural procedure for performing a local linear analysis in disks is to decompose the perturbations into shwaves, as we have done.

Eliassen, Høiland, & Riis (1953) consider both stable and unstable atmospheres and analyze an initial-value problem by decomposing the perturbations in time via Laplace transforms.¹⁵ For flow between two parallel walls, they find that an arbitrary initial disturbance behaves asymptotically as $t^{(\alpha-1)/2}$ for $-3/4 < \text{Ri} < 1/4$, where

$$\alpha \equiv \sqrt{1 - 4 \text{Ri}}, \quad (61)$$

which grows algebraically for $\text{Ri} < 0$. The disturbance grows exponentially only for $\text{Ri} < -3/4$. For a semi-infinite flow, the power-law behavior in time holds for $-2 < \text{Ri} < 1/4$, with exponential growth for $\text{Ri} < -2$. These results illustrate the importance of boundary conditions in determining stability.

In the $k_z = 0$ limit that we are concerned with here, the correspondence between the disk and atmospheric models turns out to be exact in the shwave formalism. This is because the Coriolis force only appears in equation (56) via $\tilde{\kappa}^2$, which disappears when $k_z = 0$. The equation describing the time evolution of shwaves in both a radially-stratified disk and a shearing, stratified atmosphere is thus

$$\tilde{k}^2 \ddot{\delta v}_x + 4\tilde{q}\Omega \tilde{k}_x k_y \dot{\delta v}_x + k_y^2 (N_x^2 + 2\tilde{q}^2 \Omega^2) \delta v_x = 0. \quad (62)$$

We analyze the solutions to this equation in the following section.

4.3. Solutions

Changing time variables in equation (62) to $\tilde{\tau} \equiv \tilde{k}_x/k_y$, the differential equation governing δv_x becomes

$$(1 + \tilde{\tau}^2) \frac{d^2 \delta v_x}{d\tilde{\tau}^2} + 4\tilde{\tau} \frac{d\delta v_x}{d\tilde{\tau}} + (\text{Ri} + 2) \delta v_x = 0. \quad (63)$$

The solutions to equation (63) are hypergeometric functions. With the change of variables $z \equiv -\tilde{\tau}^2$, equation (63) becomes

$$z(1-z) \frac{d^2 \delta v_x}{dz^2} + \frac{1-5z}{2} \frac{d\delta v_x}{dz} - \frac{\text{Ri}+2}{4} \delta v_x = 0. \quad (64)$$

¹⁵Cited in Miles (1961).

The hypergeometric equation (Abramowitz & Stegun 1972)

$$z(1-z)\frac{d^2\delta v_x}{dz^2} + [c - (a+b+1)z]\frac{d\delta v_x}{dz} - ab\delta v_x = 0 \quad (65)$$

has as its two linearly independent solutions $F(a, b; c; z)$ and $z^{1-c}F(a - c + 1, b - c + 1; 2 - c; z)$. Comparison of equations (64) and (65) shows that $a = (3 - \alpha)/4$, $b = (3 + \alpha)/4$ and $c = 1/2$, where α is defined in equation (61).

The general solution for δv_x is thus given by

$$\delta v_x = C_1 F\left(\frac{3-\alpha}{4}, \frac{3+\alpha}{4}; \frac{1}{2}; -\tilde{\tau}^2\right) + C_2 \tilde{\tau} F\left(\frac{5-\alpha}{4}, \frac{5+\alpha}{4}; \frac{3}{2}; -\tilde{\tau}^2\right), \quad (66)$$

where C_1 and C_2 are constants of integration representing the two degrees of freedom in our reduced system. These two degrees of freedom can be represented physically by the initial velocity and displacement of a perturbed fluid particle in the radial direction. The radial Lagrangian displacement ξ_x is obtained from equation (66) by direct integration,¹⁶

$$\xi_x = \int \delta v_x dt = -\frac{C_2}{\tilde{q}\Omega\text{Ri}} F\left(\frac{1-\alpha}{4}, \frac{1+\alpha}{4}; \frac{1}{2}; -\tilde{\tau}^2\right) + \frac{C_1}{\tilde{q}\Omega} \tilde{\tau} F\left(\frac{3-\alpha}{4}, \frac{3+\alpha}{4}; \frac{3}{2}; -\tilde{\tau}^2\right). \quad (67)$$

The solutions for the other perturbation variables can be obtained from equations (51), (52) and (53) with $k_z = 0$:

$$\delta v_y = -\tilde{\tau} \delta v_x, \quad (68)$$

$$\frac{\delta \Sigma}{\Sigma_0} = \frac{\xi_x}{L_S} \quad (69)$$

and

$$\frac{\delta P}{P_0} = \frac{\gamma\Omega}{ic_s k_y} \left[\tilde{q} \tilde{\tau} \frac{d}{d\tilde{\tau}} \left(\frac{\delta v_x}{c_s} \right) + 2(\tilde{q} - 1) \frac{\delta v_x}{c_s} \right]. \quad (70)$$

It can be seen from the latter equation and the solution for δv_x that $\delta P/P_0$ remains small compared to $\delta v_x/c_s$ in the short-wavelength limit. This demonstrates the consistency of the Boussinesq approximation.

The hypergeometric functions can be transformed to a form valid for large $\tilde{\tau}$ (see Abramowitz & Stegun 1972 equations 15.3.7 and 15.1.1). An equivalent form of the solution for $|\tilde{\tau}| \gg 1$ is

$$\begin{aligned} \delta v_x = & (C_1 V_1 + \text{sgn}(\tilde{\tau}) C_2 V_2) |\tilde{\tau}|^{\frac{\alpha-3}{2}} F\left(\frac{3-\alpha}{4}, \frac{5-\alpha}{4}; 1 - \frac{\alpha}{2}; -\frac{1}{\tilde{\tau}^2}\right) + \\ & (C_1 V_3 + \text{sgn}(\tilde{\tau}) C_2 V_4) |\tilde{\tau}|^{-\frac{\alpha+3}{2}} F\left(\frac{3+\alpha}{4}, \frac{5+\alpha}{4}; 1 + \frac{\alpha}{2}; -\frac{1}{\tilde{\tau}^2}\right), \end{aligned} \quad (71)$$

¹⁶In our notation, a subscript x or y on the symbol ξ indicates a Lagrangian displacement, not a component of the potential vorticity, which is a scalar.

where $\text{sgn}(\tilde{\tau})$ is the arithmetic sign of $\tilde{\tau}$ and the constants V_i are given by

$$\begin{aligned} V_1 &\equiv \frac{\Gamma\left(\frac{1}{2}\right)\Gamma\left(\frac{\alpha}{2}\right)}{\Gamma\left(\frac{3+\alpha}{4}\right)\Gamma\left(-\frac{1-\alpha}{4}\right)}, \quad V_2 \equiv \frac{\Gamma\left(\frac{3}{2}\right)\Gamma\left(\frac{\alpha}{2}\right)}{\Gamma\left(\frac{5+\alpha}{4}\right)\Gamma\left(\frac{1+\alpha}{4}\right)}, \\ V_3 &\equiv \frac{\Gamma\left(\frac{1}{2}\right)\Gamma\left(-\frac{\alpha}{2}\right)}{\Gamma\left(\frac{3-\alpha}{4}\right)\Gamma\left(-\frac{1+\alpha}{4}\right)}, \quad V_4 \equiv \frac{\Gamma\left(\frac{3}{2}\right)\Gamma\left(-\frac{\alpha}{2}\right)}{\Gamma\left(\frac{5-\alpha}{4}\right)\Gamma\left(\frac{1-\alpha}{4}\right)}. \end{aligned} \quad (72)$$

Expanding the above form of the solution for $|\tilde{\tau}| \gg 1$, we obtain

$$\delta v_x = (C_1 V_1 + \text{sgn}(\tilde{\tau}) C_2 V_2) |\tilde{\tau}|^{\frac{\alpha-3}{2}} + (C_1 V_3 + \text{sgn}(\tilde{\tau}) C_2 V_4) |\tilde{\tau}|^{-\frac{\alpha+3}{2}} + O(\tilde{\tau}^{-2}). \quad (73)$$

An equivalent form of ξ_x for $|\tilde{\tau}| \gg 1$ is

$$\begin{aligned} \xi_x &= \left(-\frac{C_2 X_1}{\tilde{q} \Omega \text{Ri}} + \text{sgn}(\tilde{\tau}) \frac{C_1 X_2}{\tilde{q} \Omega} \right) |\tilde{\tau}|^{\frac{\alpha-1}{2}} F\left(\frac{3-\alpha}{4}, \frac{1-\alpha}{4}; 1 - \frac{\alpha}{2}; -\frac{1}{\tilde{\tau}^2}\right) + \\ &\quad \left(-\frac{C_2 X_3}{\tilde{q} \Omega \text{Ri}} + \text{sgn}(\tilde{\tau}) \frac{C_1 X_4}{\tilde{q} \Omega} \right) |\tilde{\tau}|^{-\frac{\alpha+1}{2}} F\left(\frac{3+\alpha}{4}, \frac{1+\alpha}{4}; 1 + \frac{\alpha}{2}; -\frac{1}{\tilde{\tau}^2}\right), \end{aligned} \quad (74)$$

where the constants X_i are given by

$$\begin{aligned} X_1 &\equiv \frac{\Gamma\left(\frac{1}{2}\right)\Gamma\left(\frac{\alpha}{2}\right)}{\Gamma\left(\frac{1+\alpha}{4}\right)\Gamma\left(\frac{1+\alpha}{4}\right)}, \quad X_2 \equiv \frac{\Gamma\left(\frac{3}{2}\right)\Gamma\left(\frac{\alpha}{2}\right)}{\Gamma\left(\frac{3+\alpha}{4}\right)\Gamma\left(\frac{3+\alpha}{4}\right)}, \\ X_3 &\equiv \frac{\Gamma\left(\frac{1}{2}\right)\Gamma\left(-\frac{\alpha}{2}\right)}{\Gamma\left(\frac{1-\alpha}{4}\right)\Gamma\left(\frac{1-\alpha}{4}\right)}, \quad X_4 \equiv \frac{\Gamma\left(\frac{3}{2}\right)\Gamma\left(-\frac{\alpha}{2}\right)}{\Gamma\left(\frac{3-\alpha}{4}\right)\Gamma\left(\frac{3-\alpha}{4}\right)}. \end{aligned} \quad (75)$$

Expanding ξ_x for $|\tilde{\tau}| \gg 1$ yields

$$\xi_x = \left(-\frac{C_2 X_1}{\tilde{q} \Omega \text{Ri}} + \text{sgn}(\tilde{\tau}) \frac{C_1 X_2}{\tilde{q} \Omega} \right) |\tilde{\tau}|^{\frac{\alpha-1}{2}} + \left(-\frac{C_2 X_3}{\tilde{q} \Omega \text{Ri}} + \text{sgn}(\tilde{\tau}) \frac{C_1 X_4}{\tilde{q} \Omega} \right) |\tilde{\tau}|^{-\frac{\alpha+1}{2}} + O(\tilde{\tau}^{-2}). \quad (76)$$

The dominant contribution for each perturbation variable at late times is thus

$$\delta P \propto \delta v_x \sim t^{\frac{\alpha-3}{2}}, \quad (77)$$

$$\delta \Sigma \propto \xi_x \sim t^{\frac{\alpha-1}{2}}, \quad (78)$$

and

$$\delta v_y \propto t \delta v_x \sim t^{\frac{\alpha-1}{2}}. \quad (79)$$

This leads to one of our main conclusions: the density and y -velocity perturbations will grow asymptotically for $\alpha > 1$, i.e. $\text{Ri} \propto N_x^2 < 0$.¹⁷ For small Richardson number, however (as is

¹⁷Notice that this is the same time dependence obtained by Eliassen, Høiland, & Riis (1953) in a modal analysis; see the discussion surrounding equation (61). These power law time-dependences can be obtained more efficiently by solving the large- $\tilde{\tau}$ limit of equation (66).

expected for a Keplerian disk with modest radial gradients), $\alpha \sim 1 - 2\text{Ri}$ and the asymptotic growth is extremely slow:

$$\delta\Sigma \sim \delta v_y \sim t^{-\text{Ri}}. \quad (80)$$

In the stratified shearing sheet, the right-hand side of equation (5) governing the evolution of the perturbed potential vorticity is no longer zero. The form of this equation for the incompressive shwaves is

$$\dot{\delta\xi} = \frac{d}{dt} \left(\frac{i\tilde{k}_x \delta v_y - ik_y \delta v_x}{\Sigma_0} \right) = \frac{c_s^2 k_y}{iL_P \Sigma_0^2} \delta\Sigma. \quad (81)$$

The asymptotic time dependence of the perturbed potential vorticity can be obtained by integrating equation (81):

$$\delta\xi \sim t^{\frac{\alpha+1}{2}} \sim t^{1-\text{Ri}} \quad (82)$$

for $\tilde{\tau} \gg 1$ and $|\text{Ri}| \ll 1$. As noted in §2, an entropy gradient is not required to generate vorticity. For $N_x^2 = 0$, $\alpha = 1$ and the perturbed potential vorticity grows linearly with time. The unstratified shearing sheet is recovered in the limit of zero stratification ($1/L_P \rightarrow 0$), since in this limit equation (81) reduces to $\xi = \text{constant}$.

4.4. Energetics of the Incompressive Shwaves

For a physical interpretation of the incompressive shwaves in the stratified shearing sheet, we repeat the analysis of section 3.3 for the solution given in the previous section. For a complete description of the energy in this case, however, we must include the potential energy of a fluid element displaced in the radial direction. Following Miles (1961), an expression for the energy in the Boussinesq approximation is obtained by summing equation (46) multiplied by δv_x and equation (47) multiplied by δv_y . Replacing $\delta\Sigma/\Sigma_0$ by ξ_x/L_S via equation (69) results in the following expression for the energy evolution:

$$\frac{dE_k}{d\tilde{\tau}} \equiv \frac{d}{d\tilde{\tau}} \left(\frac{1}{2} \Sigma_0 \delta v^2 + \frac{1}{2} \Sigma_0 N_x^2 \xi_x^2 \right) = \Sigma_0 \delta v_x \delta v_y, \quad (83)$$

where $\delta v^2 = \delta v_x^2 + \delta v_y^2$. The three terms in equation (83) can be identified as the kinetic energy, potential energy and Reynolds stress associated with an individual shwave. One may readily verify that the vortical shwaves (see equations (24)-(26)) in the unstratified shearing sheet ($N_x^2 = 0$) satisfy equation (83).

The right hand side of equation (83) can be rewritten $-\tilde{\tau} \delta v_x^2$ and individual trailing shwaves ($\tilde{\tau} > 0$) are therefore associated with a negative angular momentum flux. If the energy were positive definite this would require that individual shwaves always decay. But when $N_x^2 < 0$ ($\text{Ri} < 0$) the potential energy associated with a displacement is negative, so the energy E_k can be negative and a negative angular momentum flux is not enough to halt shwave growth.

Our next step is to write the constants of integration C_1 and C_2 in terms of the initial radial velocity and displacement of the shearing wave, δv_{x0} and ξ_{x0} :

$$C_1 = \frac{\tilde{q}\Omega \text{Ri} \delta v_{x2}(\tilde{\tau}_0) \xi_{x0} + \xi_{x1}(\tilde{\tau}_0) \delta v_{x0}}{\delta v_{x1}(\tilde{\tau}_0) \xi_{x1}(\tilde{\tau}_0) + \text{Ri} \delta v_{x2}(\tilde{\tau}_0) \xi_{x2}(\tilde{\tau}_0)}, \quad C_2 = \frac{-\tilde{q}\Omega \text{Ri} \delta v_{x1}(\tilde{\tau}_0) \xi_{x0} + \text{Ri} \xi_{x2}(\tilde{\tau}_0) \delta v_{x0}}{\delta v_{x1}(\tilde{\tau}_0) \xi_{x1}(\tilde{\tau}_0) + \text{Ri} \delta v_{x2}(\tilde{\tau}_0) \xi_{x2}(\tilde{\tau}_0)}, \quad (84)$$

where $\tilde{\tau}_0 = k_{x0}/k_y$, δv_{x1} is the hypergeometric function given by equation (66) with $C_1 = 1$ and $C_2 = 0$, and the other functions are similarly defined. These expressions can be simplified by noticing that the denominator of C_1 and C_2 is the Wronskian of the differential equation for ξ_x :¹⁸

$$(1 + \tilde{\tau}^2) \frac{d^2 \xi_x}{d\tilde{\tau}^2} + 2\tilde{\tau} \frac{d\xi_x}{d\tilde{\tau}} + \text{Ri} \xi_x = 0. \quad (85)$$

The Wronskian of this equation is

$$\mathcal{W} \equiv \frac{d\xi_{x2}}{d\tilde{\tau}} \xi_{x1} - \frac{d\xi_{x1}}{d\tilde{\tau}} \xi_{x2} = \exp \left(- \int^{\tilde{\tau}} \frac{2\tau^2}{1 + \tau^2} d\tau \right) = \frac{1}{1 + \tilde{\tau}^2}. \quad (86)$$

We further simplify the analysis by setting the initial displacement ξ_{x0} to zero.

With these simplifications, the solution given by equations (66) and (67) becomes

$$\begin{aligned} \frac{\delta v_x}{\delta v_{x0}} = (1 + \tilde{\tau}_0^2) & \left[F \left(\frac{1 - \alpha}{4}, \frac{1 + \alpha}{4}; \frac{1}{2}; -\tilde{\tau}_0^2 \right) F \left(\frac{3 - \alpha}{4}, \frac{3 + \alpha}{4}; \frac{1}{2}; -\tilde{\tau}^2 \right) + \right. \\ & \left. \text{Ri} \tilde{\tau}_0 F \left(\frac{3 - \alpha}{4}, \frac{3 + \alpha}{4}; \frac{3}{2}; -\tilde{\tau}_0^2 \right) \tilde{\tau} F \left(\frac{5 - \alpha}{4}, \frac{5 + \alpha}{4}; \frac{3}{2}; -\tilde{\tau}^2 \right) \right], \end{aligned} \quad (87)$$

$$\begin{aligned} \frac{\xi_x}{\delta v_{x0}} = (1 + \tilde{\tau}_0^2) & \left[-\frac{1}{\tilde{q}\Omega} \tilde{\tau}_0 F \left(\frac{3 - \alpha}{4}, \frac{3 + \alpha}{4}; \frac{3}{2}; -\tilde{\tau}_0^2 \right) F \left(\frac{1 - \alpha}{4}, \frac{1 + \alpha}{4}; \frac{1}{2}; -\tilde{\tau}^2 \right) + \right. \\ & \left. \frac{1}{\tilde{q}\Omega} F \left(\frac{1 - \alpha}{4}, \frac{1 + \alpha}{4}; \frac{1}{2}; -\tilde{\tau}_0^2 \right) \tilde{\tau} F \left(\frac{3 - \alpha}{4}, \frac{3 + \alpha}{4}; \frac{3}{2}; -\tilde{\tau}^2 \right) \right]. \end{aligned} \quad (88)$$

As in section 3.3, the energy integral for the incompressive perturbations is given by

$$\langle E_i \rangle = \frac{1}{2} \Sigma_0 L^2 \int k_0 dk_0 \langle \delta v_{\perp}^2(k_0) \rangle \int_0^{2\pi} d\theta \sin^2 \theta \left[(1 + \tilde{\tau}^2) \left(\frac{\delta v_x}{\delta v_{x0}} \right)^2 + N_x^2 \left(\frac{\xi_x}{\delta v_{x0}} \right)^2 \right], \quad (89)$$

for initial perturbations perpendicular to and isotropic in \mathbf{k}_0 . Changing integration variables to $\tilde{\tau} = \tilde{q}\Omega t + \cot \theta$, the angular integral becomes

$$\begin{aligned} 2 \int_{-\infty}^{\infty} d\tilde{\tau} & \left[(1 + \tilde{\tau}^2) \{ \xi_{x1}(\tilde{\tau} - \tilde{q}\Omega t) \delta v_{x1}(\tilde{\tau}) + \text{Ri} \xi_{x2}(\tilde{\tau} - \tilde{q}\Omega t) \delta v_{x2}(\tilde{\tau}) \}^2 + \right. \\ & \left. \text{Ri} \{ \xi_{x2}(\tilde{\tau} - \tilde{q}\Omega t) \xi_{x1}(\tilde{\tau}) - \xi_{x1}(\tilde{\tau} - \tilde{q}\Omega t) \xi_{x2}(\tilde{\tau}) \}^2 \right], \end{aligned} \quad (90)$$

¹⁸Based upon the relationship between a hypergeometric function and its derivatives, $\delta v_{x1} = d(\xi_{x1})/d\tilde{\tau}$ and $\text{Ri} \delta v_{x2} = -d(\xi_{x2})/d\tilde{\tau}$.

where we have used the relation $\sin \theta = (1 + \tilde{\tau}_0^2)^{-1}$. In the limit of large $\tilde{q}\Omega t$, the dominant contribution to the angular integral comes from the region $0 \lesssim \tilde{\tau} \lesssim \tilde{q}\Omega t$. This can be seen from the following argument. Using the expansions given by equations (73) and (76), we find the angular integrand is

$$2|\tilde{\tau}(\tilde{\tau} - \tilde{q}\Omega t)|^{\alpha-1} [(V_1 X_1 + \text{sgn}(\tilde{\tau}) \text{sgn}(\tilde{\tau} - \tilde{q}\Omega t) \text{Ri} V_2 X_2)^2 + \text{Ri} X_1^2 X_2^2 (\text{sgn}(\tilde{\tau}) - \text{sgn}(\tilde{\tau} - \tilde{q}\Omega t))^2] \quad (91)$$

for $|\tilde{\tau}| \gg 1$ and $|\tilde{\tau} - \tilde{q}\Omega t| \gg 1$. Using the relation $\Gamma(n+1) = n\Gamma(n)$, one can easily show that

$$X_2 = \frac{2}{\alpha-1} V_1 \quad \text{and} \quad V_2 = \frac{2}{\alpha+1} X_1. \quad (92)$$

The integrand therefore simplifies to

$$|\tilde{\tau}(\tilde{\tau} - \tilde{q}\Omega t)|^{\alpha-1} V_1^2 X_1^2 \frac{2}{1-\alpha} [\text{sgn}(\tilde{\tau}) - \text{sgn}(\tilde{\tau} - \tilde{q}\Omega t)]^2, \quad (93)$$

which is zero unless $0 < \tilde{\tau} < \tilde{q}\Omega t$ (for $t > 0$). For large $\tilde{q}\Omega t$, therefore, the angular integral is approximately given by

$$\frac{16V_1^2 X_1^2}{1-\alpha} \int_{\nu}^{\tilde{q}\Omega t - \nu} d\tilde{\tau} [\tilde{\tau}(\tilde{\tau} - \tilde{q}\Omega t)]^{\alpha-1} = \frac{16V_1^2 X_1^2}{\alpha(1-\alpha)} \frac{(\tilde{\tau}\tilde{q}\Omega t)^{\alpha}}{\tilde{q}\Omega t} F\left(\alpha, 1-\alpha; 1+\alpha; \frac{\tilde{\tau}}{\tilde{q}\Omega t}\right) \Big|_{\nu}^{\tilde{q}\Omega t - \nu}, \quad (94)$$

where $1 \ll \nu \ll \tilde{q}\Omega t$. For $\tilde{q}\Omega t \gg \nu$, the above expression can be approximated by evaluating it at $\tilde{\tau} = \tilde{q}\Omega t$, giving

$$\langle E_i(\tilde{q}\Omega t \gg 1) \rangle \simeq 16V_1^2 X_1^2 \frac{\Gamma(1+\alpha)\Gamma(\alpha)}{\alpha(1-\alpha)\Gamma(2\alpha)} (\tilde{q}\Omega t)^{2\alpha-1} \langle E_i(t=0) \rangle, \quad (95)$$

where we have used equation 15.3.7 in Abramowitz & Stegun (1972) to evaluate $F(a, b; c; 1)$.¹⁹

Notice that there is no power-law growth in the perturbation energy for $\text{Ri} > 1/4$,²⁰ consistent with the classical Richardson criterion (60). In our analysis the energy decays with time for $2\alpha - 1 < 0$, or $\text{Ri} > 3/16$. Thus the energy of an initial isotropic set of incompressive perturbations in a radially-stratified shearing sheet-model grows asymptotically (for $\text{Ri} < 3/16$), just like the compressive shwaves and *unlike* the incompressive shwaves in an unstratified shearing sheet, for which the energy is constant in time.

The growth of an ensemble of incompressive shwaves in a stratified disk is *not* due to a Rayleigh-Taylor or convective type instability. There is asymptotic growth for $0 < \text{Ri} < 3/16$, and convective instability requires $\text{Ri} < 0$. One can also see this by examining the asymptotic energy for small values of $|\text{Ri}|$, such as would be expected for a Keplerian disk with modest radial gradients:

$$\langle E_i(\tilde{q}\Omega t \gg 1) \rangle \simeq [2\pi^2 \text{Ri} + O(\text{Ri}^2)] \tilde{q}\Omega t^{1-4\text{Ri}+O(\text{Ri}^2)} \langle E_i(t=0) \rangle. \quad (96)$$

¹⁹We have numerically integrated the angular integral (90) and found this to be an excellent approximation at late times.

²⁰For $\text{Ri} > 1/4$, α is imaginary and $\text{Re}[t^{2\alpha-1}] = t^{-1} \cos(2|\alpha| \ln t)$.

Evidently for small values of Ri the near-linear growth in time of the energy is independent of the sign of Ri and therefore N_x^2 .²¹

5. Implications

We have studied the nonaxisymmetric linear theory of a thin, radially-stratified disk. Our findings are: (i) incompressive, short-wavelength perturbations in the unstratified shearing sheet exhibit transient growth and asymptotic decay, but the energy of an ensemble of such shwaves is constant with time (consistent with Afshordi, Mukhopadhyay, & Narayan 2004); (ii) short-wavelength compressive shwaves grow asymptotically in the unstratified shearing sheet, as does the energy of an ensemble of such shwaves, which in the absence of any other dissipative effects (e.g., radiative damping) will result in a compressive shwave steepening into a train of weak shocks; (iii) incompressive shwaves in the stratified shearing sheet have density and azimuthal velocity perturbations $\delta\Sigma$, $\delta v_y \sim t^{-\text{Ri}}$ (for $|\text{Ri}| \ll 1$); (iv) incompressive shwaves in the stratified shearing sheet are associated with an angular momentum flux proportional to $-\tilde{k}_x/k_y$; leading shwaves therefore have positive angular momentum flux and trailing shwaves have negative angular momentum flux; (v) the energy of an ensemble of incompressive shwaves in the stratified shearing sheet behaves asymptotically as $t^{1-4\text{Ri}}$ for $|\text{Ri}| \ll 1$. For Keplerian disks with modest radial gradients, $|\text{Ri}|$ is expected to be $\ll 1$, and there will therefore be weak growth in a single shwave for $\text{Ri} < 0$ and near-linear growth in the energy of an ensemble of shwaves, independent of the sign of Ri .

Along the way we have found the following solutions: (i) an exact solution for non-vortical shwaves in the unstratified shearing sheet, equations (14), (15) and (20); (ii) a WKB-solution for the non-vortical, compressive shwaves in the short-wavelength, high-frequency limit, equations (34)-(36); (iii) a solution for incompressive shwaves in the unstratified shearing sheet valid in the short-wavelength, low-frequency limit, equations (24)-(26); (iv) a solution for incompressive shwaves in the radially-stratified shearing sheet (also valid in the short-wavelength, low-frequency limit), equations (66)-(70).

Our results are summarized in Figure 1, which shows the regions of amplification and decay for shwaves in a stratified disk in the $N_x^2/\Omega, \tilde{q}$ plane.

The presence of power-law growth of incompressive shwaves in stratified disks opens the possibility of a transition to turbulence as amplified shwaves enter the nonlinear regime. Any such transition would depend, however, on the nonlinear behavior of the disk after the shwaves break. It is far from clear that they would continue to grow. We will evaluate the nonlinear behavior of the disk in subsequent work.

Our results are essentially in agreement with the numerical results presented by Klahr (2004)

²¹This asymptotic expression assumes $\text{Ri} \neq 0$. Notice that the energy at late times can have the opposite sign to the initial energy because the potential energy is negative for $N_x^2 < 0$.

(although the decay of high frequency, compressive shwaves seen in his Figures 8, 9, 10 is likely a numerical effect since compressive shwaves grow asymptotically in our analysis), that is, we find that arbitrarily large amplification factors can be obtained by starting with appropriate initial conditions. Our results, however, clarify the nature and asymptotic time dependence of the growth. Our results on the unstratified shearing sheet are also consistent with the results of Afshordi, Mukhopadhyay, & Narayan (2004), who find that an isotropic ensemble of incompressive shwaves have fixed energy.

This work was supported by NSF grant AST 00-03091 and a Drickamer Fellowship for BMJ. We thank Jeremy Goodman for his comments.

We demonstrate here that the Boussinesq approximation to the linear perturbation equations is formally equivalent to a short-wavelength, low-frequency limit of the full set of linear equations. We perform the demonstration for the stratified shearing-sheet model since the standard shearing sheet is recovered in the limit of zero stratification.

Combining equations (45) through (49) into a single equation for δv_x yields the following differential equation, fourth-order in time:

$$F_4 \delta v_x^{(4)} + F_3 \delta v_x^{(3)} + F_2 \delta v_x^{(2)} + F_1 \delta v_x^{(1)} + F_0 \delta v_x = 0, \quad (1)$$

where

$$F_4 = \tilde{k}_x^2 \left[(k_y^2 + k_z^2) \left(1 - \frac{i}{\tilde{k}_x L_P} \right)^2 + k_y^2 \frac{2(\tilde{q}+1)(\tilde{q}+2)}{\tilde{k}_x^2 H^2} \right], \quad (2)$$

$$F_3 = -2\tilde{q}\Omega \tilde{k}_x k_y (k_y^2 + k_z^2) \left(1 + \frac{i}{\tilde{k}_x L_P} \right), \quad (3)$$

$$F_2 = c_s^2 \tilde{k}_x^2 \left[\tilde{k}_x^2 \left(1 + \frac{1}{\tilde{k}_x^2 L_P^2} + \frac{N_x^2 + \tilde{\kappa}^2}{\tilde{k}_x^2 H^2} \right) \left\{ (k_y^2 + k_z^2) \left(1 - \frac{i}{\tilde{k}_x L_P} \right)^2 + k_y^2 \frac{2(\tilde{q}+1)(\tilde{q}+2)}{\tilde{k}_x^2 H^2} \right\} + (k_y^2 + k_z^2) \left\{ (k_y^2 + k_z^2) \left(1 - \frac{i}{\tilde{k}_x L_P} \right)^2 + k_y^2 \frac{2(\tilde{q}+1)(3\tilde{q}+2)}{\tilde{k}_x^2 H^2} \right\} \right], \quad (4)$$

$$F_1 = 4\tilde{q}\Omega c_s^2 k_y \tilde{k}_x^3 \left[(k_y^2 + k_z^2) \left(1 + \frac{i}{\tilde{k}_x L_P} \right) \left\{ 1 + \frac{i(3\tilde{q}-2)}{2\tilde{q}\tilde{k}_x L_P} + \frac{\tilde{\kappa}^2}{4\tilde{q}\tilde{k}_x^2 L_P^2} - \frac{N_x^2 + \tilde{\kappa}^2}{2\tilde{k}_x^2 H^2} \right\} + 3k_y^2 \frac{(\tilde{q}+1)(\tilde{q}+2)}{\tilde{k}_x^2 H^2} \left(1 - \frac{2i}{3\tilde{q}\tilde{k}_x L_P} \right) \right], \quad (5)$$

$$F_0 = c_s^2 \tilde{k}_x^2 \left[k_y^2 (N_x^2 + 2\tilde{q}^2 \Omega^2) + k_z^2 (N_x^2 + \tilde{\kappa}^2) \right] \left[(k_y^2 + k_z^2) \left(1 - \frac{i}{\tilde{k}_x L_P} \right)^2 + k_y^2 \frac{2(\tilde{q}+1)(3\tilde{q}+2)}{\tilde{k}_x^2 H^2} \right]. \quad (6)$$

The above expressions have been written to make the short-wavelength limit more apparent: all but the leading-order terms in brackets are proportional to factors of $(\tilde{k}_x L_P)^{-1}$ or $(\tilde{k}_x H)^{-1}$. Notice also that since one expects $H/L_P \ll 1$ for Keplerian disks with modest radial gradients,

$$\frac{1}{\tilde{k}_x L_P} = \frac{1}{k_y H \tilde{\tau}} \frac{H}{L_P} \ll \frac{1}{k_y H \tilde{\tau}}, \quad (7)$$

(for $\tilde{\tau} \neq 0$) and therefore the short-wavelength limit is sufficient. One needs to be careful in taking this limit, however, since $\tilde{k}_x = k_y \tilde{\tau}$ goes through zero as a shwave goes from leading to trailing. The approximation is rigorously valid only for $\tilde{\tau} \neq 0$, but we have numerically integrated the full

set of linear equations (equations (45) through (49) with $k_z = 0$) and found good agreement with the Boussinesq solutions described in §4.3 for all $\tilde{\tau}$ at sufficiently short wavelengths.²²

With these assumptions in mind, to leading order in $(Hk_y)^{-1}$ equation (1) becomes

$$\begin{aligned} \tilde{k}_x \delta v_x^{(4)} - 2\tilde{q}\Omega k_y \delta v_x^{(3)} + c_s^2 \tilde{k}_x \tilde{k}^2 \delta v_x^{(2)} + 4\tilde{q}\Omega c_s^2 \tilde{k}_x^2 k_y \delta v_x^{(1)} + \\ c_s^2 \tilde{k}_x [k_y^2 (N_x^2 + 2\tilde{q}^2 \Omega^2) + k_z^2 (N_x^2 + \tilde{\kappa}^2)] \delta v_x = 0. \end{aligned} \quad (8)$$

If we assume $\partial_t \ll c_s k_y$, the two highest-order time derivatives are of lower order and can be neglected (thereby eliminating the compressive shwaves) and we have

$$\tilde{k}^2 \delta \ddot{v}_x + 4\tilde{q}\Omega \tilde{k}_x k_y \delta \dot{v}_x [k_y^2 (N_x^2 + 2\tilde{q}^2 \Omega^2) + k_z^2 (N_x^2 + \tilde{\kappa}^2)] \delta v_x = 0. \quad (9)$$

This is equivalent to equation (56).

Notice also that the assumption $\partial_t \sim O(c_s k_y)$ applied to equation (8) yields

$$\delta v_x^{(4)} + c_s^2 \tilde{k}^2 \delta v_x^{(2)} = 0 \quad (10)$$

to leading order in $(Hk_y)^{-1}$. This equation is of the same form as the short-wavelength limit of equation (16) for the compressive shwaves in the unstratified shearing sheet, confirming our claim that short-wavelength compressive shwaves are unchanged at leading order by stratification.

²²One must start with a set of initial conditions consistent with equations (46), (47), (51) and (52) in order to accurately track the incompressive-shwave solutions. In addition, suppression of the high-frequency compressive-shwave solutions near $\tilde{\tau} = 0$ requires $k_y L_P \gtrsim 200$, which for $H/L_P = 0.1$ implies $Hk_y \gtrsim 20$.

REFERENCES

Abramowitz, M. & Stegun, I. A. 1972, Handbook of Mathematical Functions, New York: Dover, 1972

Afshordi, N., Mukhopadhyay, B., & Narayan, R. 2004, ArXiv Astrophysics e-prints, astro-ph/0412194

Balbus, S. A. 1988, ApJ, 324, 60

Balbus, S. A. & Hawley, J. F. 1991, ApJ, 376, 214

Balbus, S. A. & Hawley, J. F. 1998, Reviews of Modern Physics, 70, 1

Balbus, S. A., Hawley, J. F., & Stone, J. M. 1996, ApJ, 467, 76

Blaes, O. M. 1987, MNRAS, 227, 975

Cabot, W. 1984, ApJ, 277, 806

Chagelishvili, G. D., Zahn, J.-P., Tevzadze, A. G., & Lominadze, J. G. 2003, A&A, 402, 401

Chimonas, G. 1970, J. Fluid Mech., 43, 833

Eliassen, A., Høiland, E., & Riis, E. 1953, Two-Dimensional Perturbation of a Flow with Constant Shear of a Stratified Fluid, Institute for Weather and Climate Research, Norwegian Academy of Sciences and Letters, Publ. no. 1

Gammie, C. F. & Menou, K. 1998, ApJ, 492, L75

Goldreich, P., Goodman, J., & Narayan, R. 1986, MNRAS, 221, 339

Goldreich, P. & Lynden-Bell, D. 1965, MNRAS, 130, 125

Goldreich, P. & Tremaine, S. 1978, ApJ, 222, 850

Goodman, J., Narayan, R., & Goldreich, P. 1987, MNRAS, 225, 695

Hawley, J. F. 1991, ApJ, 381, 496

Hawley, J.F., Gammie, C.F., & Balbus, S.A. 1995, ApJ, 440, 742

Hawley, J. F., Gammie, C. F., & Balbus, S. A. 1996, ApJ, 464, 690

Houghton, J. T. 2002, The Physics of Atmospheres, 3rd ed., Cambridge, UK: Cambridge University Press, 2002

Howard, L. N. 1961, Journal of Fluid Mechanics, 10, 509

Jeffreys, H. 1930, Proc. Cambridge Phil. Soc., 26, 170

Julian, W. H. & Toomre, A. 1966, *ApJ*, 146, 810

Klahr, H. H. & Bodenheimer, P. 2003, *ApJ*, 582, 869 (KB03)

Klahr, H. 2004, *ApJ*, 606, 1070

Knobloch, E. & Spruit, H. C. 1986, *A&A*, 166, 359

Lovelace, R. V. E., Li, H., Colgate, S. A., & Nelson, A. F. 1999, *ApJ*, 513, 805

Li, H., Finn, J. M., Lovelace, R. V. E., & Colgate, S. A. 2000, *ApJ*, 533, 1023

Li, H., Colgate, S. A., Wendroff, B., & Liska, R. 2001, *ApJ*, 551, 874

Menou, K. 2000, *Science*, 288, 2022

Miles, J. W. 1961, *Journal of Fluid Mechanics*, 10, 496

Narayan, R., Goldreich, P., & Goodman, J. 1987, *MNRAS*, 228, 1

Papaloizou, J. C. B. & Pringle, J. E. 1984, *MNRAS*, 208, 721

Papaloizou, J. C. B. & Pringle, J. E. 1985, *MNRAS*, 213, 799

Papaloizou, J. C. B. & Pringle, J. E. 1987, *MNRAS*, 225, 267

Pedlosky, J. 1979, *Geophysical Fluid Dynamics*, New York: Springer-Verlag, 1979

Spiegel, E. A. & Veronis, G. 1960, *ApJ*, 131, 442

Stone, J. M. & Balbus, S. A. 1996, *ApJ*, 464, 364

Stone, J. M., Gammie, C. F., Balbus, S. A., & Hawley, J. F. 2000, *Protostars and Planets IV*, 589

Stone, J. M. & Norman, M. L. 1992, *ApJS*, 80, 753

Toomre, A. 1969, *ApJ*, 158, 899

Umurhan, O. M. & Regev, O. 2004, *A&A*, 427, 855

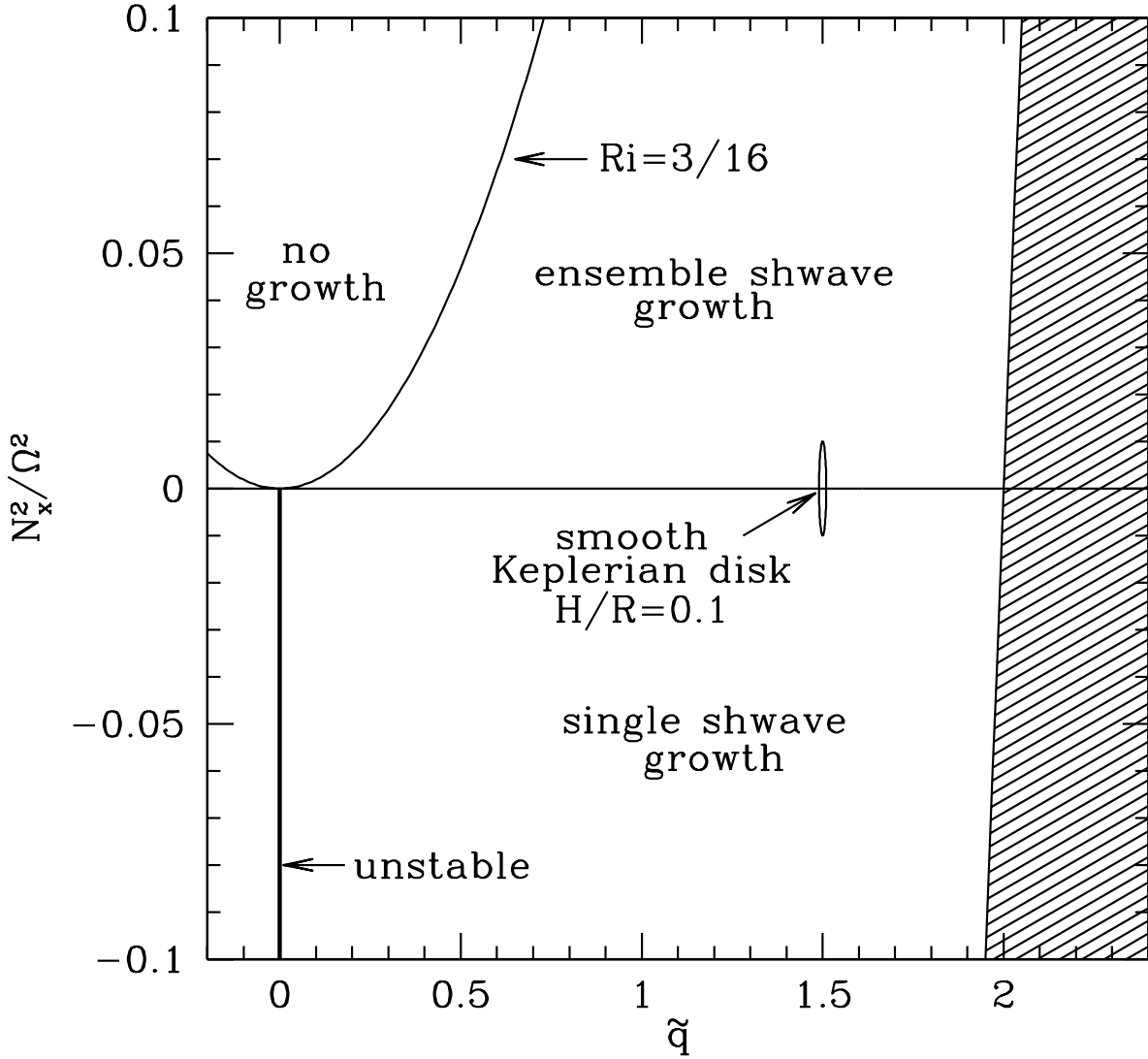


Fig. 1.— A summary of analytic results for shwaves (shearing waves) in a stratified disk. The relevant parameters are the local shearing rate $\tilde{q} = -\frac{1}{2}d \ln \Omega^2 / d \ln r$ and the dimensionless Brunt-Väisälä frequency N_x^2/Ω^2 . The expected location of a thin, smooth disk is shown as a vertically extended ellipse near $\tilde{q} = 0$, $N_x^2/\Omega^2 = 0$. The far right region (shaded in the figure) is forbidden by the Høiland criterion. When $\tilde{q} = 0$ shear is absent and a modal analysis is possible; instability is present for $N_x^2 < 0$. Solitary shwaves with $\text{Ri} = N_x^2/(\tilde{q}^2 \Omega^2) < 0$ experience asymptotic power-law growth ($\propto t^{-\text{Ri}}$ for small Ri); since each shwave grows the energy of an ensemble of shwaves does as well. For $0 < \text{Ri} < 3/16$ solitary shwaves decay but the energy of an ensemble of shwaves grows as a power-law in time. For $\text{Ri} > 3/16$ both solitary shwaves and the energy of an ensemble of shwaves asymptotically decay.